TKI 2022

Numerical Investigation of Hurricane-Induced Failure of a Military Tent

Krzysztof KOSIUCZENKO

Military Institute of Armour and Automotive Technology
Sulejówek, Poland; e-mail: krzysztof.kosiuczenko@witpis.eu

The subject of this research was the analysis of a numerical case of catastrophic destruction of a large-area military tent under the influence of a hurricane impact. As a result of the research, the level of the destructive load was identified, and the construction failure process was reconstructed. The practical effect of the work was the conclusion on the reinforcement of the structure. The calculations were made using the finite element method in the LS Dyna calculation program.

Keywords: FEM; finite element method; strength; tent hall; wind.

1. Introduction

The term catastrophic failure refers to a total, sudden and often unexpected failure of construction, which results in irreversible changes in its main performance parameters. The issues of such catastrophes are mainly analysed in construction, including the design process of the large-area tent halls.

In the analysis of the risk of a catastrophic failure, a significant place is occupied by one of the main investigative procedures which is the genesis procedure of previous disasters. As a result of the genesis procedure, the development of the adverse operational event is elaborated. The analysis contains the answer to two key questions, how and why the event occurred [7].

The development of modern simulation methods enables detailed verification of the accepted hypotheses, and at a later stage also, the simulation of the course of the event and a detailed description of the event's causes.

The main goal of this work was to determine the causes and the course of the catastrophic failure of a military tent. This case was interesting among others because the construction of the tent was designed to meet high environmental requirements, which means that it should have withstood extreme weather conditions.

Analyses of past disasters, their causes and effects are conducted in numerous countries. Scientific equipment, including modern computational methods [5, 6, 8, 15, 17], is commonly used to carry out these analyses. Due to the lack of sufficient measurement data, it would not be possible to fully generate the genesis of disasters without the use of computer simulations (e.g., FEM). Elucidation of the near-ground vortex structures and flows of tornadoes in the actual environment has immense significance for meteorologists and engineers. In light of wind engineering, estimation of accurate aerodynamic force acting on the building surface is crucial to predict the failure of various, especially lightweight and portable structures.

The work was carried out using numerical tools implementing the finite element method (FEM).

2. Description of the object of study

The object of the analysis was a large-area military tent with dimensions of $6.8 \times 13 \times 4.5$ m (width $\times$ length $\times$ height) and the symbol $01.54.00001''$ (from now on, referred to as the tent) [2]. The tent consisted of a canopy and an external frame; its geometric diagram is shown in Fig. 1.
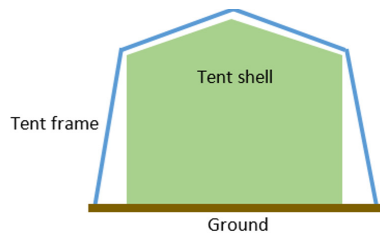
Fig. 1. Geometric diagram of the analysed tent (base 6.8×13 m).

2.1. Construction of the tent frame

The folding frame of the tent is a spatial beam structure. It consists of many beams that transmit not only axial forces (as in grill flooring), but due to the attachment of the tent shell to the frame, they also transfer all the other forces and moments. The tent's frame consisted of aluminium profiles with a rectangular cross-section of $80 \times 40 \times 3$ (horizontal) and $60 \times 60 \times 3$ (others). Their geometry is shown in Fig. 2.

Geometrical characteristics of cross-sections (moments of inertia), enabling the determination of stresses in the beams and calculated based on formulas known from the mechanics, are presented in Table 1.
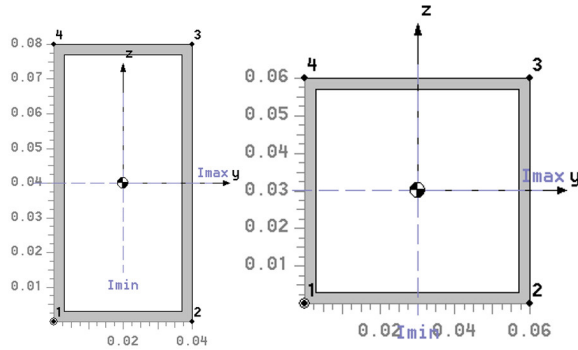
FIG. 2. Cross-sections of the frame beams: 1, 2, 3, 4-stress recovery locations (drawing and calculations by the author).

Table 1. Parameters of beam cross-sections.

Properties	Vertical beams $40 \times 80 \times 3$	Horizontal beams $60 \times 60 \times 3$
Area	$A = 0.001056$	$A = 0.000684$
Moments of inertia	$I_{zz} = 2.82112 \cdot 10^{-7}$ $I_{yy} = 1.25683 \cdot 10^{-6}$ $I_{zy} = 0$	$I_{zz} = 3.71412 \cdot 10^{-7}$ $I_{yy} = 3.71412 \cdot 10^{-7}$ $I_{zy} = 0$
Principal inertias	Max, $I_1 = 1.25683 \cdot 10^{-6}$ Min, $I_2 = 2.82112 \cdot 10^{-7}$ Polar, $I_p = 1.53894 \cdot 10^{-6}$ Angle, $\alpha = 180$	Max, $I_1 = 3.71412 \cdot 10^{-7}$ Min, $I_2 = 3.71412 \cdot 10^{-7}$ Polar, $I_p = 7.42824 \cdot 10^{-7}$ Angle, $\alpha = 90$
Radius of gyration	$y = 0.034499$ $z = 0.0163448$	$y = 0.0233024$ $z = 0.0233024$
Centroid from origin	$H = 0.02$ $V = 0.05$	$H = 0.03$ $V = 0.03$

Horizontal and vertical beams were mutually connected using bolted connections (Fig. 3).

FIG. 3. Method used to connect vertical and horizontal beams mutually.

The frame was connected to the tent canopy using webbing slings or chains (in the case of the tent roof). The tent canopy in the places of connection was

additionally reinforced with an additional layer of fabric made of polyester (PES) (Fig. 4).

FIG. 4. Connection of the frame to the tent canopy: using webbing (left) and chains (right).

The beams are made of aluminium alloy EN AW-6060 (PA38). The main material parameters of this alloy are taken from the work [1] and are listed in Table 2.

Table 2. Material parameters of the beams.

Properties	Parameter value
Young's modulus, E	69.5 GPa
Shear modulus, G	26.1 GPa
Poisson's ratio, υ	0.33
Ultimate tensile strength, R_m	Max. 240 MPa
Yield point, R_{p02}	Min. 190 MPa
Total elongation, A_5	Min. 10%
Density, ρ	2700 kg/m^3

2.2. Construction of the tent canopy

According to the technical documentation of the tent [2], the tent canopy is made of PES with a weight of 520 g/m^2, coated with a thin layer of polyvinyl chloride (PVC). Thanks to this, the canopy is characterised, for example, by good strength and high non-flammability (B1 level). The material data of the PES used for calculations (Table 3) were taken from the publicly available MatWeb database [14].

Table 3. Material parameters of the tent canopy [14].

Properties	Parameter value
Yield point, R_{p02}	228 MPa
Young's modulus, E	4.36 GPa
Ultimate tensile strength, R_m	100 MPa
Poisson's ratio, υ	0.4

2.3. Weather conditions

The destruction of the tent took place on 17–18.02.2022 as a result of the hurricane called Eunice. Weather forecasts predicted that wind velocity could exceed 120 km/h (Fig. 5). In fact, it reached a velocity of about 100 km/h.
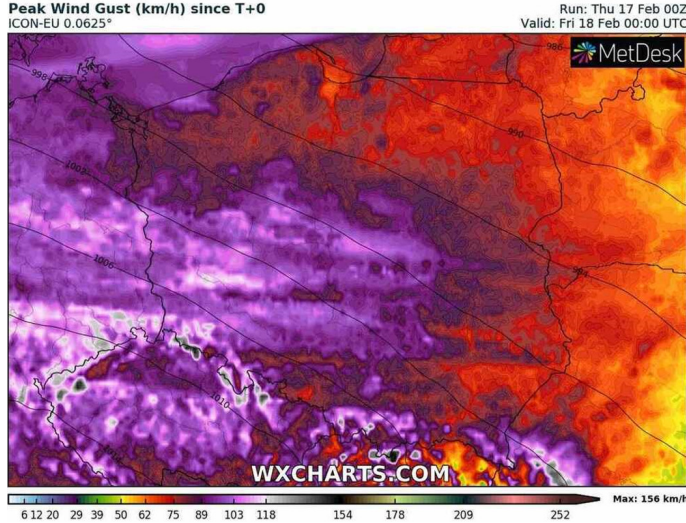
FIG. 5. Map of forecasted wind velocity in Poland created using the ICON-EU model [18].

When designing a tent to estimate the wind load of the structure, the relationship between wind velocity and wind pressure known from physics are used:

$$(2.1) \qquad p = \frac{1}{2} \cdot \rho \cdot v,$$

where ρ – air density, about 1.25 kg/m^3, v – wind velocity [m/s], and p – wind pressure.

However, the above formula leads to an unnecessary overestimation of the designed durability of the construction. Therefore, in practice, a more precise procedure described, for example, in the PN-EN 1991-1-4 standard [3], can be used. It takes into account the additional relevant factors affecting the value of the actual wind pressure, such as geographical zone (1/2/3), terrain category (0/I/II/III/IV), altitude above ground level [m] and height above sea level [m].

For example, wind pressure was calculated for a geographical point corresponding to the place of deployment of the analysed tent (Sulejówek, Poland: latitude: 52°15′07″ N, longitude 21°16′08″ E, height 104 m above sea level) at a wind velocity of 100 km/h is 426 Pa [3]. It is a value lower than 535 Pa calculated from the formula (2.1).

2.4. Recorded tent failure

As a result of the hurricane, whose wind blew at a velocity of about 100 km/h, the tent's catastrophic failure occurred (Figs. 6 and 7).

FIG. 6. Failure of the tent due to prolonged exposure to a hurricane.

FIG. 7. Visible minor damage to the frame.

The inspection of the damaged tent showed that the tent canopy was seriously destroyed (torn and slid), while the frame was damaged only to a small extent. The damage to the frame concerned only the mutual connections between the vertical and horizontal beams (Fig. 8), proving the proper selection of beam cross-sections.

FIG. 8. Bending of the frame beam connectors.

In addition to the described damage, the process of detaching the strips connecting the flaccid canopy with the rigid and more durable frame structure was also observed (Fig. 9).

FIG. 9. The connections of the frame with the tent canopy:
before the hurricane (left) and after the hurricane (right).

3. MODELLING PROCESS

The main task of the author was to develop a numerical model of the tent subjected to wind pressure load. The technical documentation showed that the tent's construction should withstand a wind pressure of 230–345 Pa, which corresponds to a wind velocity of up to 85 km/h and in gusts up to 100 km/h.

Modelling was carried out in two stages. In the first stage, a preliminary numerical model of the tent was made using the finite element method (implicit option) (Fig. 10), which was analysed in the field of nonlinear statics. Simcenter Femap 2022.1.1.40 [4] was used for this purpose. The simulation was based
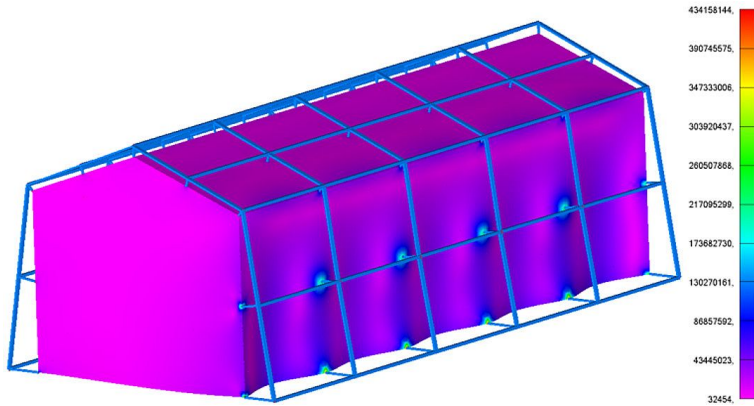
Fig. 10. Maps of stresses reduced in the tent canopy [Pa].

on the assumption of a slow increase in wind pressure. The applied material models did not consider the strain velocity's influence on the stress value. The calculations did not show that the tent could be damaged even at a wind velocity of 100 km/h. Extreme stresses appeared in the places of sewing strips connecting the frame with the canopy. However, they did not exceed 50% of the permissible stresses (up to 45 MPa). The simulation carried out in this way did not allow to identify the causes and trace the course of the catastrophic failure of the tent.

In the second stage, additional calculations were made using a more advanced computing engine. A more extensive model was prepared following the requirements of the LS Dyna programme from LSTC [9–12], using LS-PrePost control cards [13]. LS Dyna is a comprehensive tool for analysing fast-changing phenomena using the finite element method, especially the EXPLICIT type. This type of analysis is widely used in nonlinear problems and short-term collisions, e.g., explosions and plastic processing.

3.1. The applied material models

Two material models were used in the tent model: one describing the properties of the SHELL elements of the canopy and the other representing the properties of the BEAM elements of the frame. As already mentioned, the tent canopy was made of PES. Modelling the behaviour of thermoplastic materials under devastating loads is a major computational challenge. One of several material models available in the LS Dyna library is applied for polymer modelling. Models that properly simulate destruction phenomena are, e.g., MAT_81, MAT_89, MAT_101, MAT_112, MAT_141. Some available models consider thermoplasticity: MAT_60, MAT_106, MAT_168, MAT_187 [4]. There is not always a need to use these complex material models. When all the material pa-

rameters are unknown, simpler material models are used. Those models assume linear elasticity and plasticity and define simple criteria for destruction (e.g., maximum stresses or strains). The author of this work used a material model of this kind, that is, MAT_024 (full name MAT_PICEWISE_LINEAR_PLASTICITY). This model takes into account the effect of the strain rate on material properties (reinforcement), which is described by the Cowper-Symonds equations of state (constitutive):

$$(3.1) \qquad \sigma = R_e \sigma_0 \left[1 + \left(\frac{\dot{\varepsilon}}{C} \right)^{1/P} \right],$$

where C, P – coefficients of strain rate, R_e – static yield stress, ε – strain, σ_0 – static stress, σ – scaled stress resulting from the reinforcement of the material.

To model the properties of the canopy, it was assumed that the values of the parameters of the Cowper-Symonds equation are: $C = 2188$, $P = 5.5$ [16]. The remaining material parameters are presented in Table 3.

The second applied material model described the properties of the BEAM elements of the frame. The analysis of the tent frame's damage showed no plastic hinge or significant damage in it. Therefore, a simple material model MAT_03 (MAT_PLASTIC_KINEMATIC) was used to model the beams. The material parameters of the model are presented in Table 2. This model, despite its simplicity, well describes the properties after exceeding the yield point R_e (SIGY).

Similarly, the properties of other small structural elements (not belonging to the frame or canopy), such as strips, cords, and hooks, were modelled. However, in this case, the models were supplemented with the destruction criterion by adding the option of ADD_EROSION. This option made it possible to simulate the destruction of connections after exceeding, for example, the stress limit (SIGVM = 200 MPa) or strain limit (EFFEPS = 0.2).

3.2. Modelling the load of wind pressure and gravity

Modelling the action of the wind is more complicated than simply loading a surface with a constant pressure value. Simulation of the load must also take into account the turbulence and high variability over time (Fig. 11). Such variability of wind interaction may temporarily cause the wind pressure to become
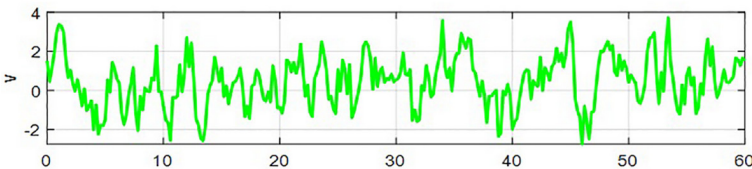
FIG. 11. Sample histogram of longitudinal wind velocity.

negative (suction phenomenon). The lower the slope of the construction, the more prominent such a suction effect is.

The simplifications were adopted for the purposes of this work and to simplify the modelled phenomenon. Those simplifications depended on the assumption that the speed and pressure of the wind changed in accordance with the function presented in Fig. 12. It was assumed that the maximum pressure ($p_{max} = 425$ Pa) and wind velocity ($v = 100$ km/h, hurricane Eunice – Fig. 5) would be achieved at the moment of $t = 1$ s and $t = 3$ s. The selection of the maximum value of wind velocity also resulted from the fact that similar values were specified in the technical documentation of the tent [2].
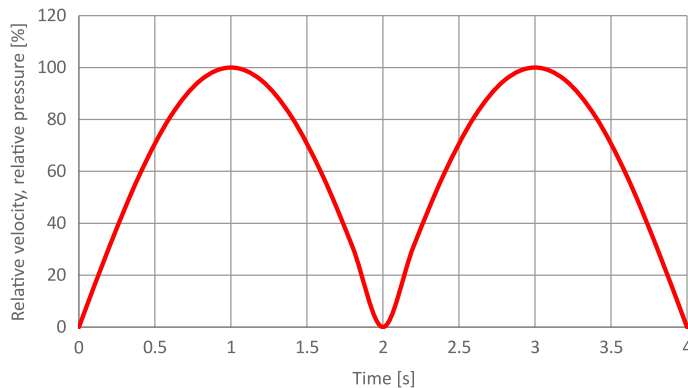
FIG. 12. The model of the time course of wind velocity and pressure adopted for further calculations (relative values v/v_{max}, p/p_{max}).

Due to the location of the tent and the partial covering of some areas of the tent by the surrounding buildings, it was assumed that the wind was blowing from the south (side of the tent) and the east (front of the tent). Therefore, only these parts of the tent canopy were subjected to load. They were realised by applying the definition of surface load LOAD_SHELL, for which the time course of the load corresponded to the course of the function in Fig. 12.

In addition to simulating wind pressure, the work considered the gravity load ($g = 9.81$ m/s²), which affected all elements of non-zero mass. This load was realised using the LOAD_BODY_Y table, in which the gravitational acceleration increased linearly from zero to 9.81 m/s² in 0.1 s. In addition, calculations were carried out with the *CONTROL_DYNAMIC_RELAXATION card switched on to stabilise gravity.

3.3. Finite element grid

The tent canopy was described with a grid of 50 000 flat finite elements of the SHELL type. In the places of predicted stress concentrations (constrictions,

holes, etc.), the density of the arrangement of elements was increased accordingly. High-quality 8-node SHELL elements were used, which allowed for obtaining more accurate results through more precise reproduction of curvatures. The displacement field in such elements is described by a parabolic function (a linear function describes the field of stresses and strains). SHELL elements were assigned the material properties from Table 3.

The aluminium frame was described with a grid of 10 000 1-dimensional BEAM elements. Depending on the needs (e.g., type of strain), the frame may be attributed to the properties based on various theories of rods (e.g., Bernoulli, Timoshenko, Vlasov). BEAM elements were assigned material properties from Table 2.

3.4. Contact modelling

The developed tent model considers the phenomenon of contact, which may occur between fragments of the tent canopy, between the tent canopy and the frame, and between the entire tent and the surface on which the tent was placed. In all these cases, contact is a nonlinear issue because the size of the contact area cannot be predicted in advance.

A SURFACE-SURFACE type contact was used to model the contact between the fragments of the tent canopy, where each node of the slave surface (SLAVE) is checked for penetration through the master surface (MASTER).

Such contact makes it possible to create pairs of surfaces that can come into contact with each other. The computing processor controls the distance between these surfaces in each computational step, and when the nodes are already close to each other, an anti-penetration force is applied. Thanks to the additional AUTOMATIC option, it was possible to automatically activate the contact without pre-indicating which surface layers would come into contact (up or down).

The NODE-SURFACE type contact was used to model the contact between the beams frame and the tent canopy. In this model, all the slave nodes (SLAVE) are controlled to see if they were not penetrated by the master surface (MASTER).

The RIGIDWALL_PLANAR contact was used to model the contact between the tent (frame and coating) and the surface. It enabled simulating of a rigid plane of the floor (ground), fixed motionlessly in space.

4. Numerical calculation results

Numerical calculations were performed in LS-Dyna on a multiprocessor computing cluster. As a result of the calculations, the resulting files were obtained. The files were the data source for the LS-PREPOST postprocessor. In this post-

processor, the results of the calculations were converted into a form convenient for evaluating the results. In analysing the course of strain and destruction of the tent, maps of reduced stresses (calculated according to the Huber-Mises-Hencky HMH energy hypothesis) generated for subsequent time moments were used (Figs. 13–17).
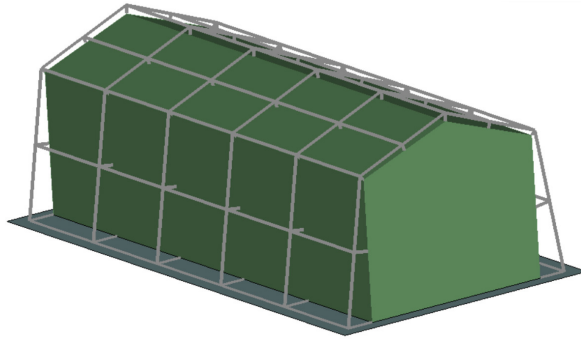
Fig. 13. View of the tent model at the moment of $t = 0$ s.
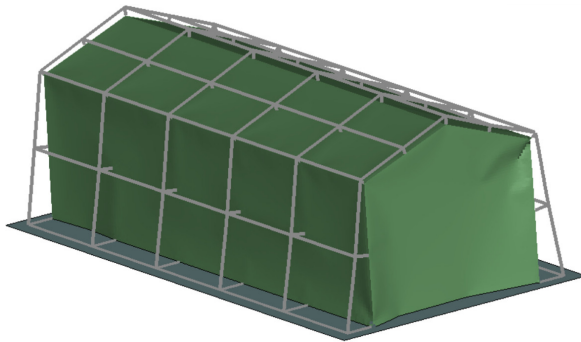
Fig. 14. View of the tent model at the moment of $t = 1$ s.
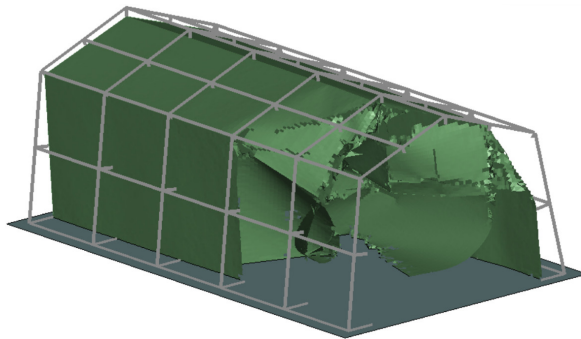
Fig. 15. View of the tent model at the moment of $t = 4$ s.

The analysis of the simulation shows that the most significant deformations occur only after damage (tearing) to the tent canopy (Figs. 16 and 17).
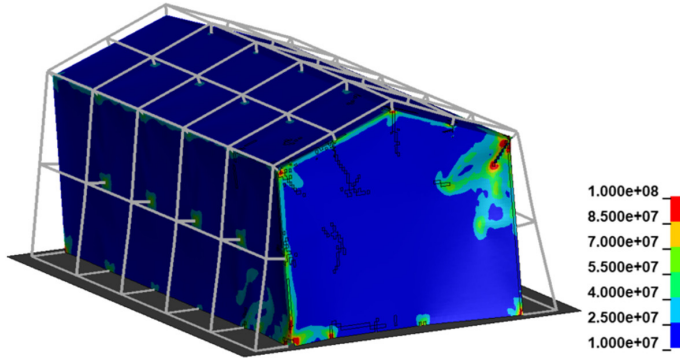
FIG. 16. The beginning of tearing the tent canopy at the moment of $t = 2.5$ s (red colour means extreme values of stress reduced [MPa].
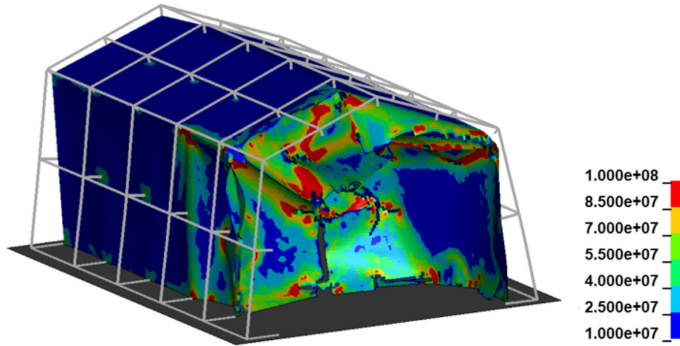
FIG. 17. The beginning of the destruction of the tent canopy at the moment of $t = 3$ s (red colour means extreme values of reduced stresses [MPa].

5. Conclusions

The main purpose of this work was to determine the causes of the catastrophic destruction of the military tent. The simulation results allowed us to trace the development of failure accurately and determine the indications to introduce specific structural changes to the tent. As a result of numerical calculations, a good correspondence was obtained between the actual observations and the model's behaviour. Observations carried out on the actual object and the presented simulation results allow us to conclude that the tent designed in accordance with applicable standards and using less advanced computational tools (FEM in the field of linear and nonlinear statics) may be destroyed under the influence of impulsive wind. In the calculations, it is necessary to use more ad-

vanced programs, e.g. LS-Dyna, which allow the model to take into account, among others, the fast and variable load, large displacements, material non-linearity, strain and structural destruction velocity. The modelling should also be preceded by an in-depth analysis of the probability of violent atmospheric phenomena occurring in the expected place of the tent (e.g. hurricanes). It was realised that the weakest link of the tent is its canopy and its connection with the frame. These elements should be made thicker or made of plastic with higher tear strength.

References

1. Abotula S., Chalivendra V., An experimental and numerical investigation of the static and dynamic constitutive behaviour of aluminium alloys, *The Journal of Strain Analysis for Engineering Design*, **45**(8): 555–565, 2010, doi: 10.1177/030932471004500808.

2. Collective work, *NUPWU new universal reusable tent hall 01.54.00001*, Rekord Hale Namiotowe, 2021.

3. EN 1991-1-4 (2005), *Eurocode 1: Actions on structures – Part 1–4: General actions – Wind actions*, Authority: The European Union Per Regulation 305/2011, Directive 98/34/EC, Directive 2004/18/EC, 2004.

4. *Femap Getting Started*, ver. 11.1, Siemens PLM, 2013.

5. Heneka P., Ruck B., A damage model for the assessment of storm damage to buildings, *Engineering Structures*, **30**(12): 3603–3609, 2008, doi: 10.1016/j.engstruct.2008.06.005.

6. Kawaguchi M., Tamura T., Mashiko W., A numerical investigation of building damage during the 6 May 2012 Tsukuba tornado using hybrid meteorological model/engineering LES method, *Journal of Wind Engineering & Industrial Aerodynamics*, **204**: 104254, 2020, doi: 10.1016/j.jweia.2020.104254.

7. Lewitowicz J., Genesis of happening maintenance and operation (exploatation) [in Polish: Genezowanie zdarzeń eksploatacyjnych], *Diagnostyka*, **3**(39): 69–78, 2006.

8. Liu Y., Ru Y., Li F., Zheng L., Zhang J., Chen X., Liang S., Structural design and optimization of separated air-rib tents based on response surface methodology, *Applied Sciences*, **31**(1): 55, 2023, doi: 10.3390/app13010055.

9. *LS-Dyna Manual Vol. I R.13.0*, Livermore Software Technology Corporation (LSTC), 2021.

10. *LS-Dyna Manual Vol. II R.13.0*, Livermore Software Technology Corporation (LSTC), 2021.

11. *LS-DYNA Support*, DYNAmore GmbH, 2022, www.dynasupport.com.

12. *LS-Dyna, Theory manual*, Livermore Software Technology Corporation, 2019.

13. *LS-PrePost Documentation*, DYNAmore GmbH, 2022, www.dynasupport.com.

14. *MatWeb's services*, 2022, www.matweb.com/index.aspx.

15. Radzka E., Olszewska E., Assessment of hazard from damaging wind gusts in the Siedlce area, *Journal of Ecological Engineering*, **23**(7): 192–196, 2022, doi: 10.12911/2299 8993/149974.

16. RAHMAN N.A., ABDULLAH S., ABDULLAH M.F., OMAR M.Z., SAJURI Z., ZAMRI W.F.H., Ballistic limit of laminated panels with different joining materials subjected to steel-hardened core projectile, *International Journal of Integrated Engineering*, **10**(5): 8–14, 2018, doi: 10.30880/ijie.2018.10.05.002.

17. VISCUSO S., DRAGOLJEVIC M., MONTICELLI C., ZANELLI A., Finite-element analysis and design optioneering of an emergency tent structure, [in:] *Proceedings of the TensiNet Symposium 2019*, A. Zanelli, C. Monticelli, M. Mollaert, B. Stimpfle [Eds.], Maggioli Editore, 2019, pp. 208–219, doi: 10.30448/ts2019.3245.42.

18. *Weather sheet WXCHART*, 2022, www.wxcharts.com [acessed: 17–18.02.2022].